Electronic Supporting Information

Design of core-shell titania-heteropolyacid-metal nanocomposites for photocatalytic reduction of CO_2 to CO at ambient temperature

Xiang Yu, Simona Moldovan, Vitaly V. Ordomsky and Andrei Y. Khodakov

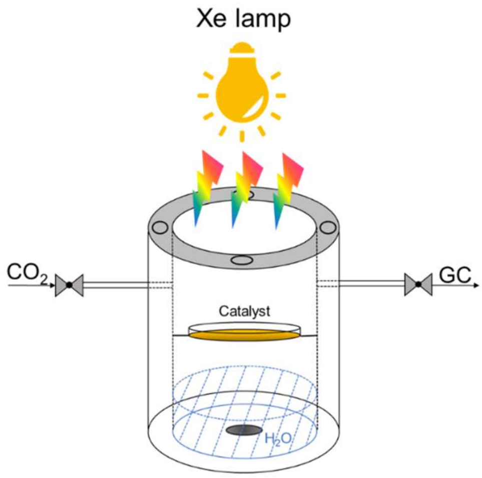

Figure S1. The schema of photocatalytic reactor

Table S1. Zn content in the Zn-HPW/TiO_2 composites from XRF.

Catalyst	Calculated Zn contents (wt.%)	Measured Zn contents (wt.%)
Zn-HPW/TiO_2	0.5	0.5
	1.5	1.6
	3.0	2.9
	6.0	6.1
	10	10.3
	12	12.2

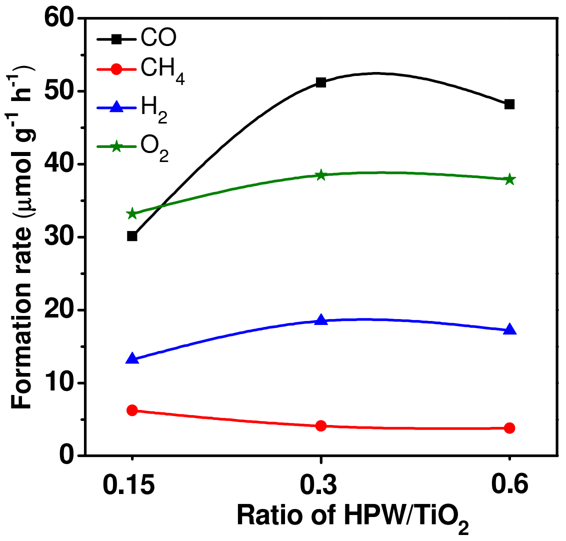

Figure S2. CO, O_2, CH_4 and H_2 formation rates over Zn-HPW/TiO_2 composites with different ratio of HPW/TiO_2. Reaction conditions: catalyst, 0.1 g; Gas phase pressure, CO_2 0.2 MPa; H_2O, 15mL; irradiation time, 6h.

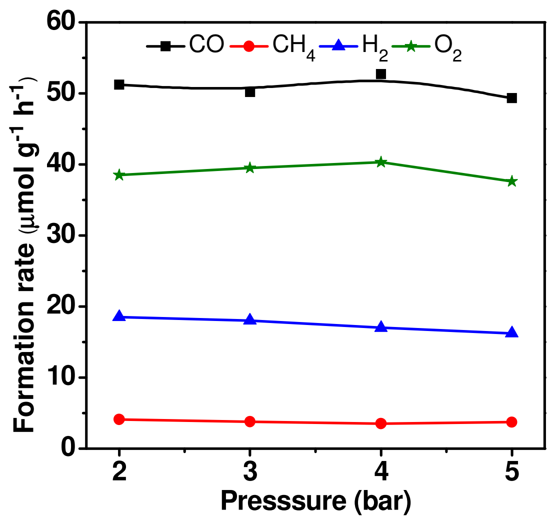

Figure S3. CO, O_2, CH_4 and H_2 formation rates over Zn-HPW/TiO_2 composites with different pressure. Reaction conditions: catalyst, 0.1 g; Gas phase pressure, CO_2 0.2 ~ 0.5 MPa; H_2O, 15mL; irradiation time, 6h.

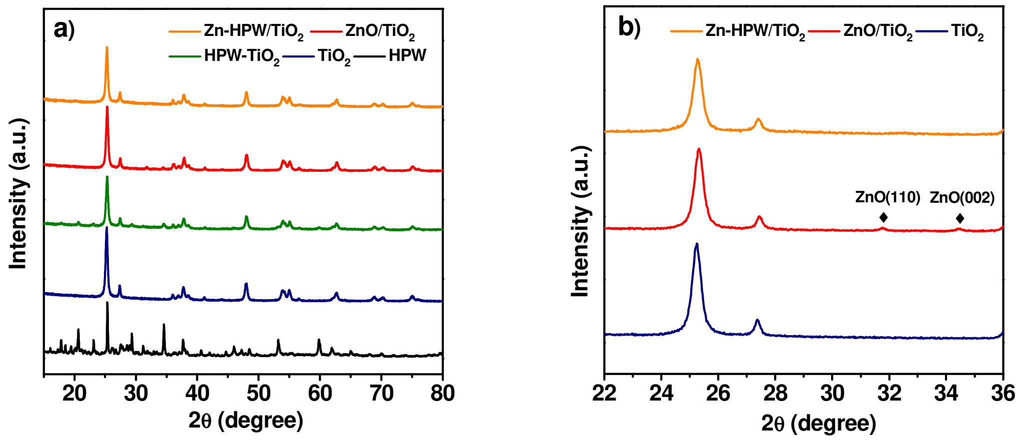

Figure S4. XRD patterns of different nanocomposites catalysts.

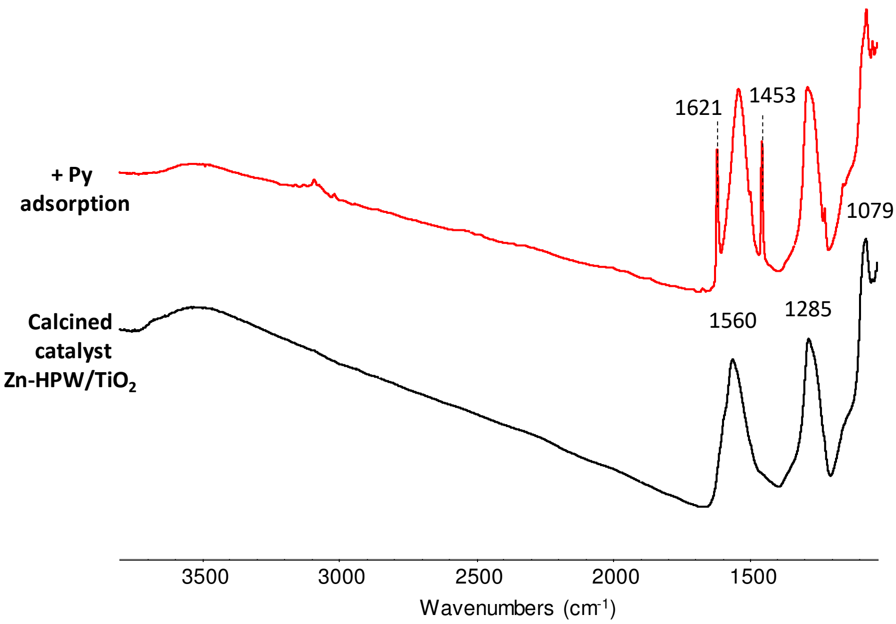

Figure S5. FTIR spectra of the calcined Zn-HPW/TiO_2 (6wt.%) catalyst before and after adsorption of pyridine on the sample dehydrated at 200°C.

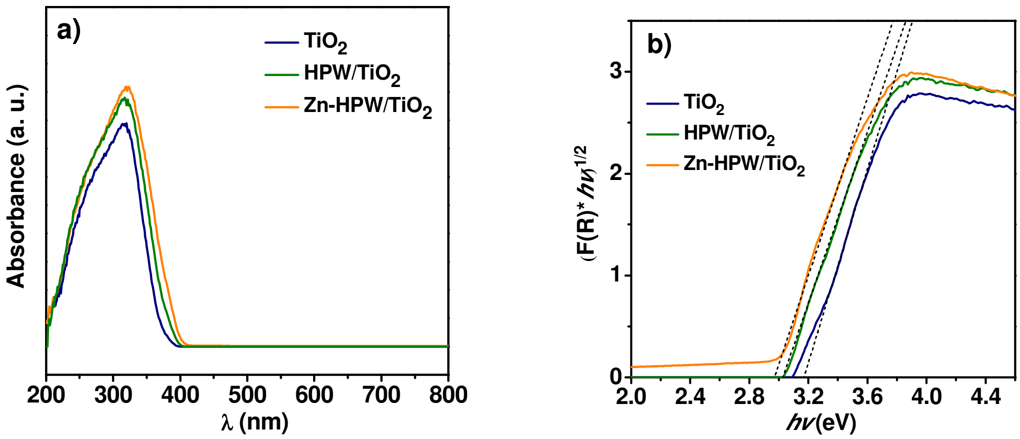

Figure S6 a. UV-Vis spectra of Zn-HPW/TiO_2 sample b. $[F(R\infty)h\nu]^{1/2}$ versus *hν* for Zn-HPW/TiO_2 sample

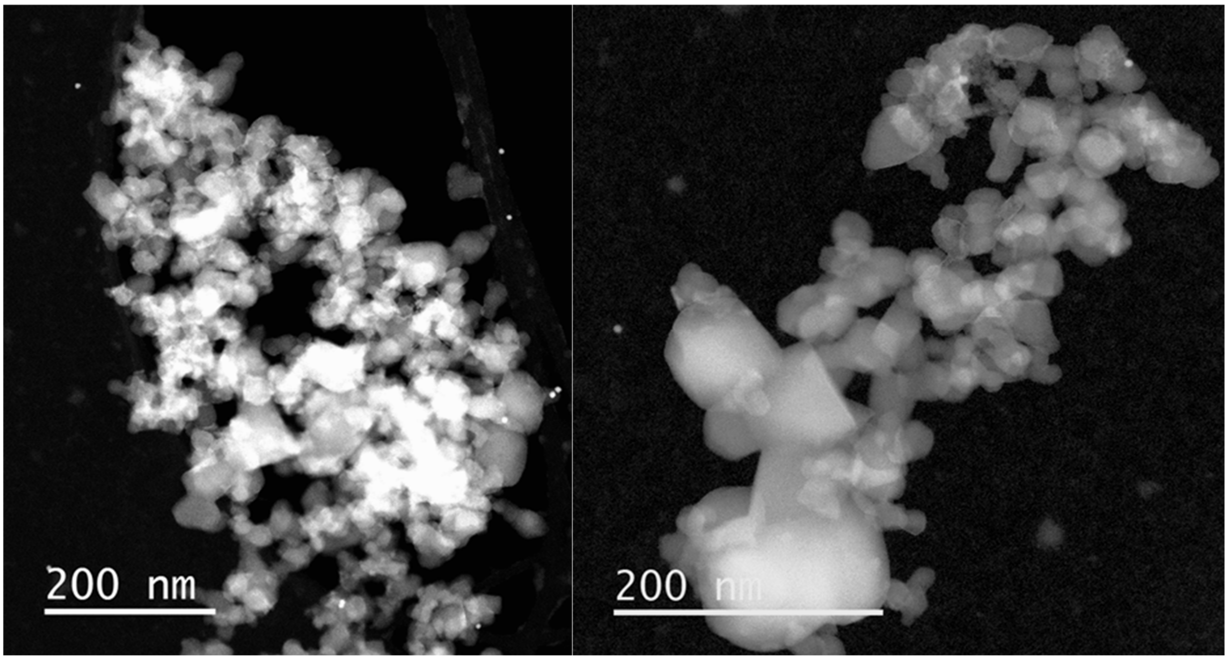

Figure S7. TEM images of the Zn-HPW/TiO_2 composite

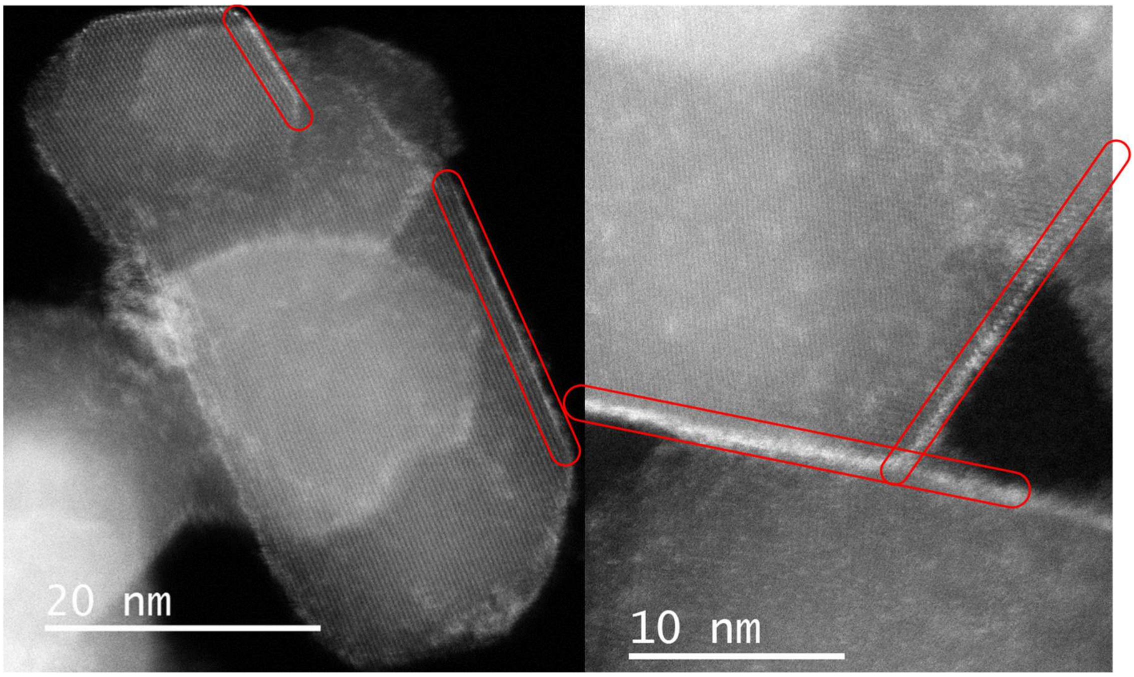

Figure S8. High resolution STEM-HAADF images showing the formation of the core shell structures in Zn-HPW/TiO_2

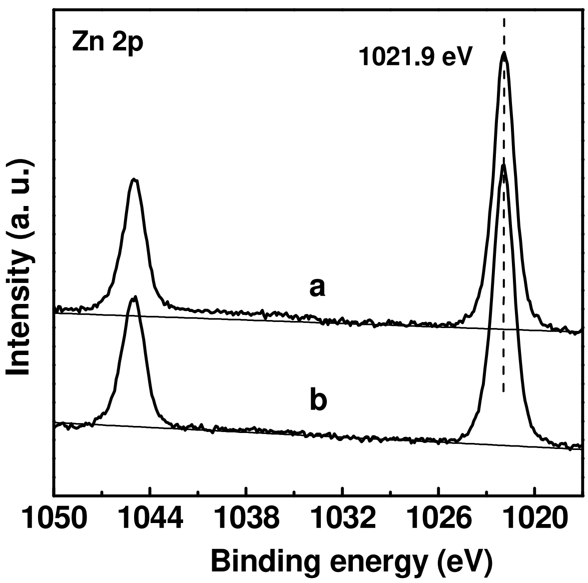

Figure S9. Zn 2p XPS spectra of Zn-HPW/TiO_2 catalysts: a. fresh catalyst, b. used catalyst.

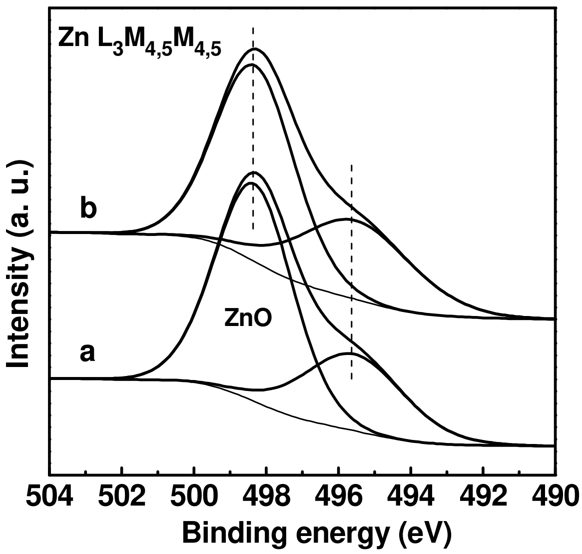

Figure S10. Zn $L_3M_{4.5}M_{4.5}$ Auger peaks for the Zn-HPW/TiO_2 catalysts; a. fresh catalyst, b. used catalyst.

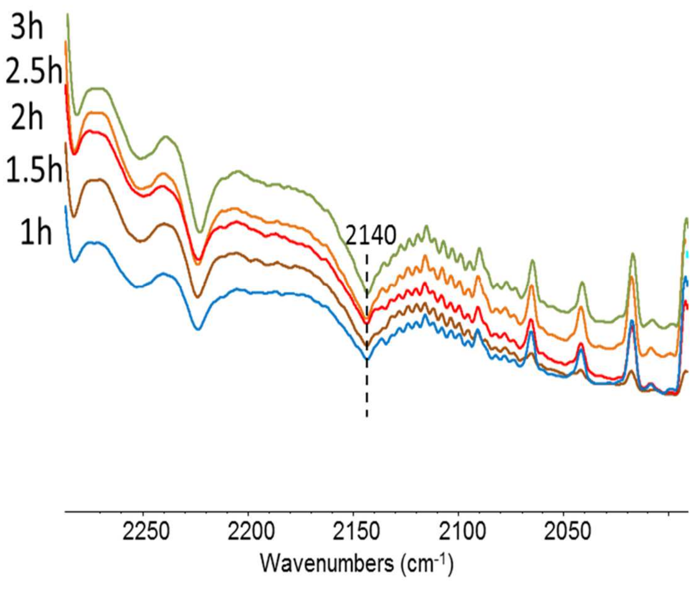

Figure S11. In situ FTIR spectra of the gas phase over the Zn-HPW/TiO_2 catalyst measured under light at different reaction times in CO_2 and H_2O vapor.